

RoboPV: A modular system for enhancing the efficiency of autonomous aerial monitoring of photovoltaic plants

Amir Mohammad Moradi Sizkouhi ^a, Mohammadreza Aghaei ^{b,c,*}, Mahdi Karimkhani ^d, Sayyed Majid Esmailifar ^d

^a Department of Electrical and Computer Engineering, Concordia University, Montreal, Canada

^b Department of Ocean Operations and Civil Engineering, Norwegian University of Science and Technology (NTNU), Ålesund, Norway

^c Department of Sustainable Systems Engineering (INATECH), Albert Ludwigs University of Freiburg, Freiburg, Germany

^d Department of Aerospace Engineering, Amirkabir University of Technology, Tehran, Iran

Keywords

Photovoltaic (PV) power plant
Autonomous aerial monitoring
Aerial robots
Encoder-decoder architecture
RoboPV

Article Info

DOI: 10.22060/aest.2025.5849

Received date 23 July 2025

Accepted date 18 August 2025

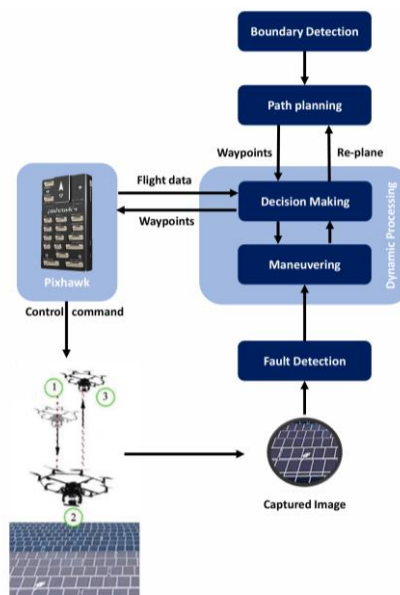
Published date 1 September 2025

* Corresponding author:
Mohammadreza.aghaei@ntnu.no

Abstract

This paper presents RoboPV, an innovative embedded software for autonomous aerial monitoring of photovoltaic (PV) plants. RoboPV automates monitoring with features like optimal trajectory planning, image processing, and real-time fault detection through four integrated components: boundary area detection, path planning, dynamic processing, and fault analysis. A specialized encoder-decoder deep learning model processes aerial images to identify plant boundaries, while a unique path planning algorithm ensures complete area coverage. During flights, a neural network analyzes images for automatic fault detection. RoboPV also includes decision-making algorithms for various flight conditions, is compatible with low-power micro-computers, and supports the MAVLink protocol for multi-rotor operations. A six-degrees-of-freedom dynamic model was tested in a SIMULINK environment, achieving 93% accuracy in autonomous inspections of large-scale PV installations.

Graphical Abstract



1. Introduction

Aerial inspections offer a rapid and reliable means of assessing the conditions of Photovoltaic (PV) systems [1]. Traditionally, human operators have been instrumental in monitoring these systems [2]. However, aerial techniques significantly improve fault diagnosis, especially for large-scale PV plants [1,3]. The failures and defects can be detected on PV modules by different sensors and special instruments [4]. In common aerial inspections, multi-rotors fly optimal paths determined by a Ground Control Station (GCS). While flight data can be collected in real-time, video streams sent to the GCS are not analyzed immediately, which limits the accuracy of monitoring since offline data analysis is still required.

In one of our previous works [5], we developed an automated control system with a dedicated multi-rotor and GCS to deliver precise insights into PV plants' performance. Additionally, a recent study utilized a CNN encoder-decoder architecture to identify potential defects in PV modules from aerial images collected through several experimental flights by multi-rotor [6]. Building on our previous research, we have created a novel PV plant monitoring software platform, "RoboPV," designed for the autonomous inspection of PV plants [7–10]. In this approach, the conventional methods have been replaced with artificial intelligence (AI)-based techniques and high-precision multi-rotors in periodic inspection missions of PV plants. By integrating AI and high-precision multi-rotors, periodic inspections of PV plants can be enhanced [1].

The proposed processing platform allows various multi-rotors to autonomously monitor large-scale PV plants while analyzing the performance and condition of PV systems. RoboPV serves as an intelligent data processing platform that can be installed on an onboard microprocessor, such as a Raspberry Pi 4, and interacts seamlessly with the 3DR Pixhawk autopilot to control different multi-rotors. By employing advanced deep learning algorithms, RoboPV significantly improves aerial inspection capabilities over traditional and semi-autonomous methods.

The platform utilizes an enhanced encoder-decoder architecture, trained with a specifically designed Fully Convolutional Network (FCN) as its foundation, to accurately detect the boundaries of PV plants. Additionally, RoboPV is equipped for automatic fault detection, analyzing real-time images to pinpoint potential issues in PV modules. To achieve this, it employs a precisely trained image segmentation model that predicts the exact location of any faults on PV modules with pixel-level precision.

The rest of this paper is structured as follows: Section 2 introduces RoboPV and outlines its construction along with how it analyzes flight data and makes decisions during aerial inspection missions. Section 3 covers the dynamic modeling of the multi-rotor used for simulation validation, and it also discusses the outcomes and performance evaluations of RoboPV in the autonomous aerial monitoring of two PV plants. Lastly, Section 4 concludes with some insights and suggestions for future research.

2. RoboPV Software Platform

Recent advancements in technology involving multi-rotors, flight controllers, and remote sensing have led to significant progress in intelligent monitoring methods. RoboPV serves as the primary processing unit within the on-board microprocessor of the aerial robot, enabling navigation of the multi-rotor during flight and facilitating real-time data analysis to enhance the efficiency of aerial monitoring for PV plants compared to conventional methods. By utilizing RoboPV, any multi-rotor can be enhanced with varying levels of intelligence, allowing for the automated inspection of entire strings of PV plants, which includes path planning, image acquisition, online image analysis for fault identification,

flight data evaluation, and decision-making for corrective actions. An automated and comprehensive embedded software suite is proposed for RoboPV, comprising four components: boundary detection, path planning, fault detection, and dynamic processing. As illustrated in **Fig. 1**, these four modules carry out the entire process of PV plant monitoring in four distinct phases:

1. **Boundary Detection:** RoboPV identifies the boundary region of the PV installation in a preliminary flight step utilizing an encoder-decoder network that is based on an FCN.
2. **Path Planning:** An optimal flight route is formulated with the shortest total distance to survey the entire PV installation using the path planning algorithm. This route is crafted according to the endurance and maneuverability of the multi-rotor.
3. **Dynamic Processing:** During the aerial inspection, the multi-rotor's flight computer collaborates with RoboPV's onboard microprocessor. RoboPV keeps track of all flight data to make decisions guided by set algorithms. If any failures in PV modules are identified during the mission, RoboPV transmits a control signal to Pixhawk to navigate the multi-rotor toward the potentially faulty area for further examination. The real-time processing evaluates the multi-rotor's capability to fulfill the mission after each maneuvering action. If required, the optimal route is re-planned for the remainder of the mission.

Fault Detection: An onboard microprocessor analyzes the video feed collected from the PV modules in real time to create feature maps pinpointing defects and failures for precise location identification.

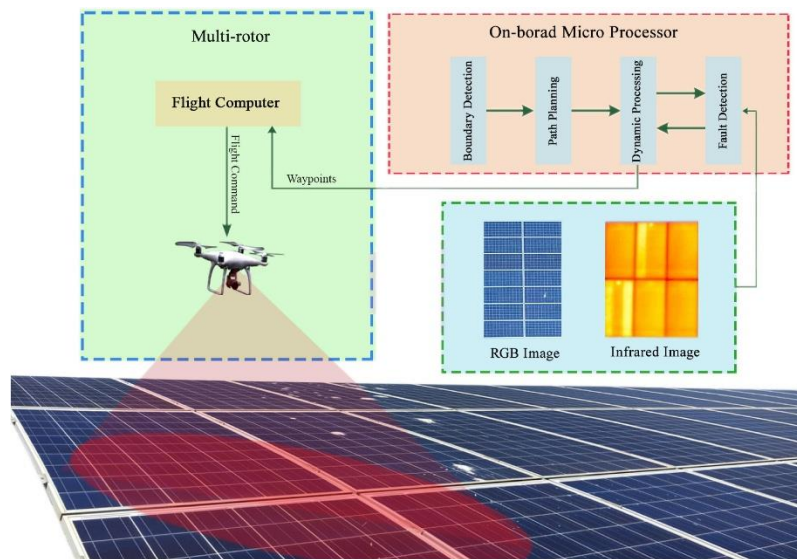


Fig. 1. An overview of the RoboPV's role in autonomous aerial monitoring of a PV plant.

2.1. Boundary Detection

As part of RoboPV, we utilize a modified FCN backbone to identify the pixel-level boundaries of a PV plant. This technique allows each pixel in the aerial image to be labeled, determining whether it is part of the PV strings. The structure of the proposed network is illustrated in **Fig. 2**.

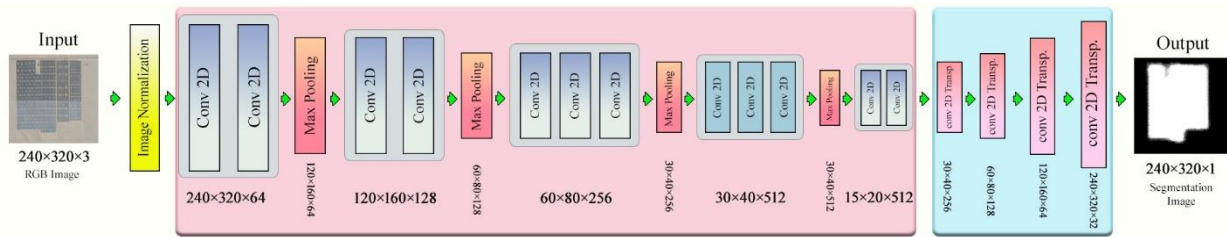


Fig. 2. The architecture of the encoder-decoder network that is used for boundary detection.

To create an accurate image segmentation model, a dataset of aerial images of large-scale photovoltaic plants, titled "Amir," was developed elsewhere [11]. A total of 3584 aerial images of PV plants from twelve different countries are included in Amir. The encoder processes these aerial images and their corresponding masks through convolutional operations to generate low-resolution feature maps. To reconstruct images featuring the extracted PV plants, these features are fed into the decoder section of the network, where up-sampling takes place. For training and evaluating the model, 80% of the entire set of images is randomly selected for the training phase, while the remaining 20% is used to assess the performance of the trained model on unseen data. The training process yields an accuracy rate of 97.61%, whereas the testing process achieves an accuracy of 96.99%. [11]. As shown in **Fig. 3**, the predictions made by the trained network are quite accurate when it comes to detecting the boundaries of three specified PV plants. The final output image measures 240 by 320 pixels, with pixel intensities ranging from 0 to 255. The model is designed to push the pixel values in the areas representing the PV plants closer to 255, which results in some regions of the image appearing gray. To delineate the boundaries of the PV plants, a threshold is established to filter the pixels based on their intensity values. For instance, pixels with values exceeding 125 are classified as parts of the PV plant boundary.



Fig. 3. Predictions of the trained model on two given PV plants.

2.2. Path Planning

In aerial autonomous monitoring of a PV plant, the multi-rotor needs to navigate a series of waypoints that encompass the entire area of the PV plant. Additionally, it is crucial to employ a dedicated path planning algorithm to calculate an optimal path for the aerial monitoring operations of the PV plants. To transmit waypoints to the aerial robot, it is necessary to precisely calculate a set of waypoints. An accurate determination of the PV plant's boundaries is vital for the path planning

algorithm. The most efficient path for the multi-rotor is one that allows for the inspection of all PV modules at the shortest distance, while ensuring that there are no blind spots within the camera's field of view (FoV), particularly in the border areas. When planning the path, the primary goal is to devise the shortest route possible within the PV plant to reduce the time taken for aerial inspections. Given the 90-degree FoV of the aerial camera utilized in this study, the multi-rotor can cover a $30 \times 30 \text{ m}^2$ area on the ground while flying at a constant altitude of 15m. The final computed flight paths are depicted with red lines over these PV plants in **Fig. 4**. By utilizing the generated optimal path, the multi-rotors will effectively cover all sections of the PV plant, with particular attention given to the corners, by the camera's FoV.

The main goal of the control block is to establish the desired waypoint for a multi-rotor based on varying flight conditions. In Home Mode, the multi-rotor launches from its home position to reach the first waypoint. In Flight Mode, it follows a predetermined path, continually updating its target waypoint as it nears the current one. In Maneuver Mode, if a fault is detected with the PV arrays, the multi-rotor will stop and descend to a height of 5 meters, hovering for 60 seconds to assess the situation. After this monitoring period, it will decide whether to continue on its current course or change its trajectory.

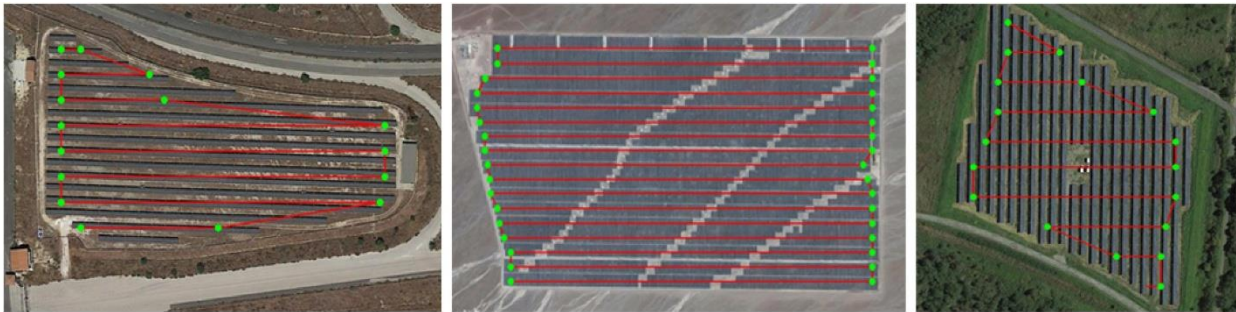


Fig. 4. The outputs of the path planning on three sample PV plants.

2.3. Dynamic Processing

RoboPV sends the calculated waypoints from the path planning to Pixhawk using an application programming interface (API) designed for MAVLink. Acting as a client, RoboPV interacts with Pixhawk through these APIs. The dynamic processing of PV plants consists of three primary subsystems, each with a specific function. Fig. 5 illustrates the schematic of the dynamic processing. As the multi-rotor operates, the dynamic processing evaluates its flight data to make rapid decisions. Flight data encompasses position, velocity, battery level, and images captured of PV strings. The dynamic processing gathers information from Pixhawk and fault detection to determine the optimal action based on the robot's current status. As shown in **Fig. 5**, this unit also engages with other elements of RoboPV and the Pixhawk flight controller. Consequently, following the evaluation of fault detection, the dynamic processing takes charge of executing maneuver actions, which include a sequence of activities for the precise inspection of the intended area. The decision-making subsystem of the dynamic processing is activated after each monitoring maneuver to assess the flight condition and make quick decisions. This phase assesses if the multi-rotor can fulfill the mission while on its current path.

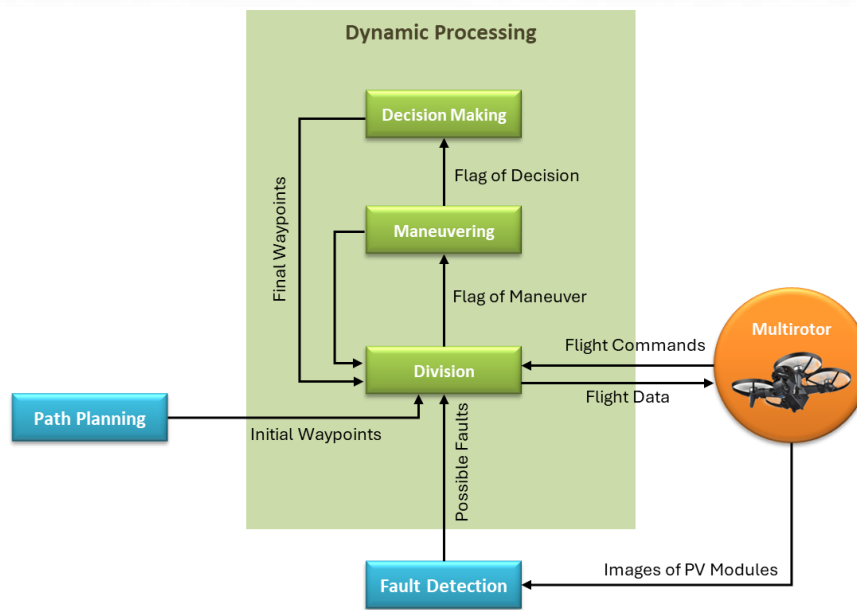


Fig. 5. The architecture of the Dynamic Processing unit.

After evaluating the potential damage to the PV modules, a maneuver command is executed. A maneuver action refers to altering the multi-rotor's states to closely inspect the target area within a PV string. During the aerial examination of a PV plant, several scenarios may arise. Initially, the damage is identified, and the multi-rotor begins its maneuvering. To approach the affected PV modules, the multi-rotor decreases its altitude. At this stage, the multi-rotor hovers at a new height to thoroughly analyze the area. After detecting the failure of a PV module, the multi-rotor ascends back to its original flight altitude and awaits further instructions from RoboPV. A key component of autonomous aerial monitoring involves decision-making. This process assesses whether the multi-rotor can proceed with its current route after each maneuver. Elevating the flight altitude is utilized to expand the multi-rotor's field of view over the ground while planning a new trajectory. By utilizing the MAVLink communication protocol, decision-making transmits the waypoints to the Pixhawk autopilot if the new altitude is viable.

2.4. Fault Detection

Once the multi-rotor starts flying over the PV plant, the fault detection unit initiates the analysis of the aerial images captured from the PV modules. Various cameras are accessible for image gathering, each with different frame rates. The multi-rotor maintains a steady cruising speed of 5 meters per second, moving forward 5 meters each second. Thus, while the fault detection unit processes the frames, the multi-rotor travels an additional 5 meters since the last time step. The movement of the multi-rotor during the image processing by the fault detection on the microprocessor does not influence the efficiency of the RoboPV in detecting faults automatically, and there is adequate overlap ($20 \times 30 \text{ m}^2$) between the images taken in the previous and current time steps.

An aerial RGB image is initially imported into a PV module extraction tool. Through various image processing methods, the module extractor identifies the modules. Utilizing a modified version of the VGG16 model, feature maps are derived from both the images and the masks. Depending on the size of the input image to the model, the first layer dimensions, known as the input layer, are adjusted accordingly.

The input images have a resolution of 640×480 pixels, and have a depth of 3. A convolutional layer is subsequently employed in the encoder unit to enlarge the dimensions of each layer. The two-dimensional matrices of the images and

masks are fed into the network as inputs. Following this, the extracted features are transmitted to the decoder section of the network for up-sampling to recreate images with bird droppings. Improved segmentation of the droppings is attained by enhancing the decoder section of the proposed encoder-decoder architecture.

The output of the trained network consists of a binary image, where the pixels identified as belonging to the multi-rotor's dropping are assigned a value of 255, while all other pixels are set to 0. To assess the network's performance, several well-established metrics were utilized, including the Dice (F1) score, the Jaccard (J) score, also known as the Intersection-Over-Union (IoU), and pixel accuracy. In segmentation tasks, the Jaccard score is particularly prevalent. This index is determined by calculating the ratio of the overlap between the predicted segmentation object and the ground truth mask to the total area of both the prediction and the ground truth combined. The training process for the neural network occurs in two stages. Initially, a down-sampling operation is performed on the images to generate low-resolution feature maps. Subsequently, an up-sampling operation is conducted to reconstruct the image, highlighting the areas where potential bird's drops may appear. A base learning rate of 0.0005 is established for the training of the network. The system provides reports on training and validation loss rates, as well as accuracy rates, at each stage of the process.

To prepare the extracted modules for training, several preprocessing steps are necessary. First, we conduct a thorough examination of each PV module to check for the presence of bird droppings. The training consists of 23 epochs, with a batch size set at 32. To ensure diversity within each batch, the images are shuffled. We utilize binary cross-entropy as our loss function. Subsequently, the encoder-decoder model is tested using the extracted modules from the PV strings to evaluate its performance. The results are illustrated in **Fig. 6**. By using a dataset that the model has not encountered during training, we find that it can accurately pinpoint the locations of bird droppings on the PV modules, achieving an impressive average accuracy of 93.33%.

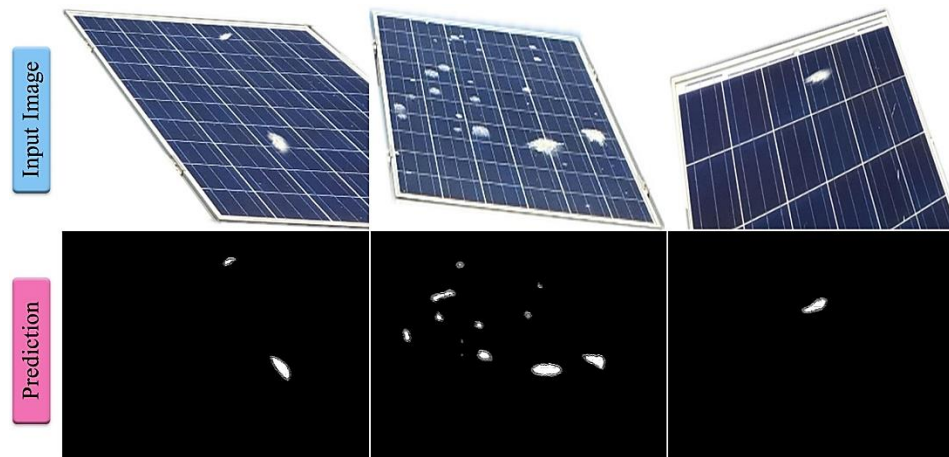


Fig. 6. The final output of the trained fault detection model for different affected PV modules by birds' drops.

Table 1. The performance measurements of the FCN with defined metrics.

No.	Activations	Pixel Accuracy	IoU Score	F1 Score
1	RELU	0.93	0.42	0.63
2	TanH	0.90	0.41	0.61
2	Sigmoid	0.95	0.46	0.62

3. Simulation and Results

In the context of model-based design for control systems, the primary requirement is the establishment of a mathematical model for the plant under consideration, which in this instance is a multi-rotor system. Multi-rotors, particularly quad-rotors, represent a highly non-linear, under-actuated, and intrinsically unstable dynamic system. They are frequently employed as test cases for control system design in several researches [12]. The flight control system encompasses various functions, including vehicle stabilization and position tracking. Within our laboratory, the Pixhawk 4, produced by Holybro, has been selected for the control of aerial vehicles across multiple operational modes, based on its performance metrics. The Pixhawk control system is comprised of three distinct cascade PID-based controllers:

1. Altitude controller: Control and change the multi-rotor's altitude by increasing or decreasing all motor angular velocity simultaneously during flight.
2. Attitude controller: Changing the multi-rotor's Euler angles by generating pitch, roll, and yaw moments.
3. Position Controller: The desired roll and pitch angles are computed and fed into the attitude controller to track the generated path via the multi-rotor.

3.1. Mathematical Modeling

To showcase the performance of RoboPV, we developed a six degrees of freedom dynamic model for a multi-rotor in a SIMULINK environment. This model was applied to an aerial monitoring mission at two different large-scale photovoltaic (PV) plants. The PIXHAWK flight control system and the SIMULINK environment were interconnected during the Hardware-in-the-Loop (HIL) test using the MAVLink API. The six degrees of freedom dynamics model, which includes both rotational and translational equations of motion for the multi-rotor, was derived based on the Euler-Newton formulas [13] as shown in **Fig. 7**.

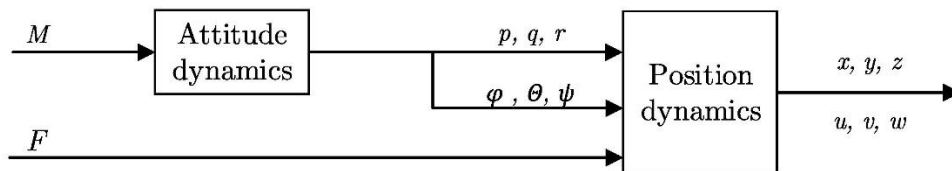


Fig. 7. Block diagram of the quadrotor's attitude and position dynamics.

3.2. Results of Monitoring

To demonstrate RoboPV's effectiveness in autonomous aerial monitoring of a PV plant, it's essential to simulate real-world conditions on the Pixhawk autopilot processor through PIL tests. For this purpose, as previously mentioned, the process begins with the boundary detection unit, which extracts the PV plant's boundary points using a trained deep neural network. These points then serve as inputs for the path planning unit. This unit, taking into account various factors such as the PV plant's dimensions, panel sizes, camera field of view (FoV), and the multi-rotor's altitude and speed, devises an optimal flight path that covers the entire plant while minimizing total distance. **Fig. 8** illustrates the processor-in-the-loop (PIL) simulation trajectories for two selected PV plants, clearly showing the multi-rotor taking off and proceeding along the pre-planned paths. The aerial robot continues its flight until it detects a potential fault. Once the fault detection unit identifies issues with the PV modules, the dynamic processing unit commands the multi-rotor to slow down and halt at the spot where the fault was detected. Subsequently, the multi-rotor descends from an altitude of 15 meters to 5 meters, hovering over the fault for 60 seconds while streaming video back to RoboPV for real-time analysis. During this time, the fault detection unit conducts a more detailed examination of the area, where the multi-rotor has lowered its altitude. After the 60 seconds have elapsed, it

automatically returns to its previous altitude and awaits further instructions from RoboPV. However, when executing fault detection maneuvers, there may be instances where the multi-rotor is unable to complete the planned trajectory due to a low state of charge (SOC). In such cases, RoboPV's decision-making unit will replan the trajectory at a higher altitude. This adjusted path results in a larger field of view but with lower accuracy, ultimately shortening the distance traveled. While this shorter trajectory ensures mission completion, it may come at the expense of performance.

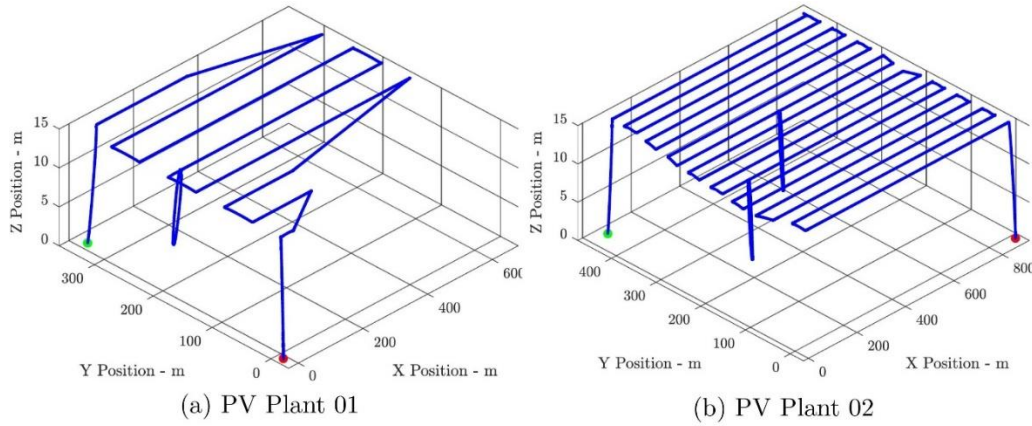


Fig. 8. The simulated aerial inspections over PV plants. (Red dot: Take-off area, Green dot: Landing area).

The detailed multi-rotor states during the simulation and the subsequent fault detection of the two mentioned PV plants are presented in Fig. 9 and Fig. 10.

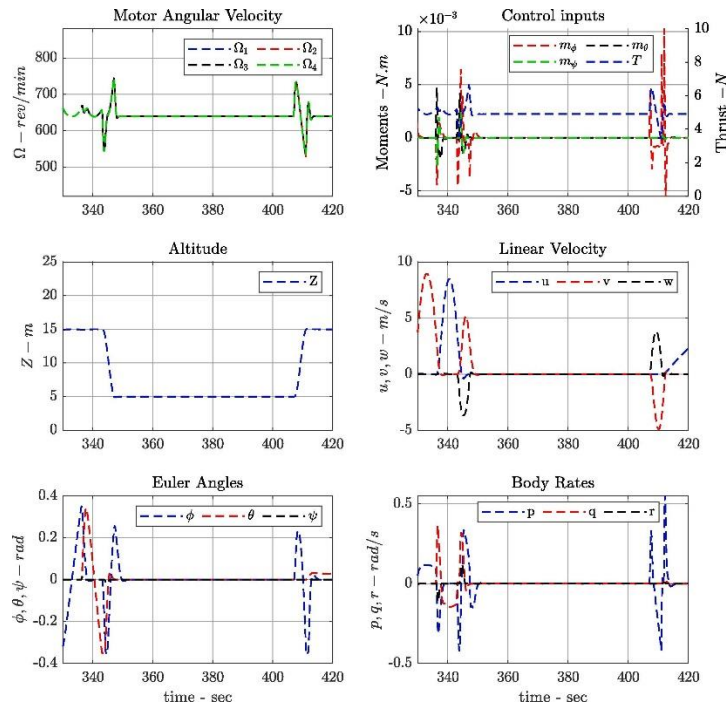


Fig. 9. Multi-rotor states during the first PV plant monitoring.

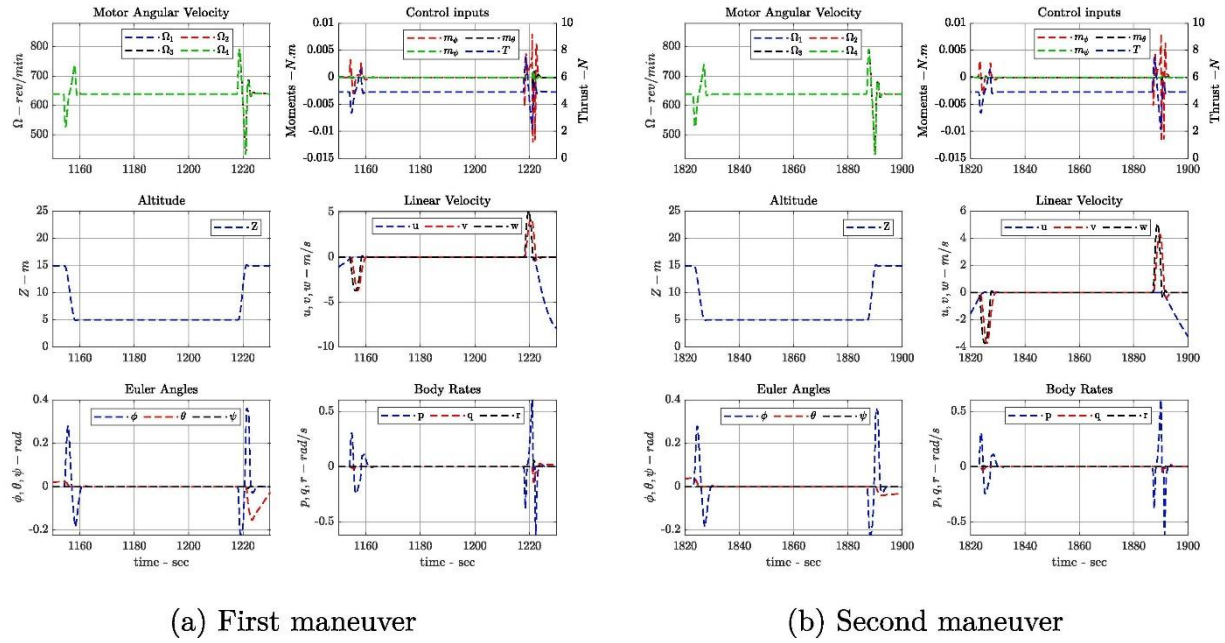


Fig. 10. Multi-rotor states during the second PV plant monitoring.

4. Conclusion

This study presents an embedded software package known as RoboPV, specifically designed for the management of aerial robots in the monitoring of large-scale PV plants. To validate the performance of RoboPV in aerial inspections, comprehensive PIL tests were conducted. The Pixhawk 4 Holybro autopilot served as the processing unit, facilitating the control and navigation of the multi-rotor along predetermined trajectories established by RoboPV. The functionalities of RoboPV—including path planning, dynamic processing, path-following guidance, and the multi-rotor dynamic model—were simulated in real time within a computer environment. The findings demonstrate that RoboPV can perform autonomous aerial inspections with an overall accuracy of 93% in large-scale PV plants. Further detailed information regarding RoboPV is available in other publications [14].

Author contributions

A.M. M.: Conceptualization, Data curation, Formal analysis, Investigation, Methodology, Software, Validation, Visualization, Writing - original draft. **M. A.:** Conceptualization, Data curation, Formal analysis, Investigation, Methodology, Resources, Supervision, Validation, Writing - review & editing. **M. K.:** Formal analysis, Investigation, Software, Visualization, Writing - review & editing. **S.M. E.:** Conceptualization, Data curation, Formal analysis, Investigation, Methodology, Resources, Supervision, Validation, Writing - review & editing.

Declaration of competing interest

The authors declare that they have no known competing financial interests or personal relationships that could have appeared to influence the work reported in this paper.

Data availability

The data that has been used is confidential.

References

- [1] M. Aghaei, M. Kolahi, A. Nedaei, N.S. Venkatesh, S.M. Esmailifar, A.M. Moradi Sizkouhi, A. Aghamohammadi, A.K.V. Oliveira, A. Eskandari, P. Parvin, J. Milimonfared, Autonomous intelligent monitoring of photovoltaic systems: An in-depth multidisciplinary review, *Prog. Photovolt. Res. Appl.* 33 (2025) 381–409.
- [2] C. Kandilli, Performance analysis of a novel concentrating photovoltaic combined system, *Energy Convers. Manag.* 67 (2013) 186–196.
- [3] M. Al-Housani, Y. Bicer, M. Koç, Experimental investigations on PV cleaning of large-scale solar power plants in desert climates: Comparison of cleaning techniques for drone retrofitting, *Energy Convers. Manag.* 185 (2019) 800–815.
- [4] M. Aghaei, M. Kolahi, A. Nedaei, N.V. Sridharan, A. Eskandari, A.K.V. De Oliveira, V. Sugumaran, R. Ruther, P. Parvin, S.M. Esmailifar, A holistic study on failures and diagnosis techniques in photovoltaic modules, components and systems, *Proc. Int. Conf. Future Energy Solutions (FES), IEEE*, (2023) 1–6.
- [5] M. Aghaei, F. Grimaccia, C.A. Gonano, S. Leva, Innovative automated control system for PV fields inspection and remote control, *IEEE Trans. Ind. Electron.* 62 (2015) 7287–7296.
- [6] A.M. Moradi Sizkouhi, M. Aghaei, S.M. Esmailifar, A deep convolutional encoder-decoder architecture for autonomous fault detection of PV plants using multi-copters, *Sol. Energy* 223 (2021) 217–228.
- [7] M. Aghaei, A. Eskandari, S. Vaezi, S.S. Chopra, Solar PV power plants, in: *Photovolt. Sol. Energy Convers.*, Elsevier, (2020) 313–348.
- [8] A.M.M. Sizkouhi, S.M. Esmailifar, M. Aghaei, A.K.V. De Oliveira, R. Ruther, Autonomous path planning by unmanned aerial vehicle (UAV) for precise monitoring of large-scale PV plants, *Proc. IEEE 46th Photovolt. Spec. Conf. (PVSC), IEEE*, (2019) 1398–1402.
- [9] A. Eskandari, J. Milimonfared, M. Aghaei, Line-line fault detection and classification for photovoltaic systems using ensemble learning model based on IV characteristics, *Sol. Energy* 211 (2020) 354–365.
- [10] A. Eskandari, J. Milimonfared, M. Aghaei, A.H.M.E. Reinders, Autonomous monitoring of line-to-line faults in photovoltaic systems by feature selection and parameter optimization of support vector machine using genetic algorithms, *Appl. Sci.* 10 (2020) 5527.
- [11] A.M.M. Sizkouhi, M. Aghaei, S.M. Esmailifar, M.R. Mohammadi, F. Grimaccia, Automatic boundary extraction of large-scale photovoltaic plants using a fully convolutional network on aerial imagery, *IEEE J. Photovolt.* 10 (2020) 1061–1067.
- [12] X. Zhang, X. Li, K. Wang, Y. Lu, A survey of modelling and identification of quadrotor robot, *Abstr. Appl. Anal.* 2014 (2014) 320526.
- [13] A.A. Najm, I.K. Ibraheem, Nonlinear PID controller design for a 6-DOF UAV quadrotor system, *Eng. Sci. Technol. Int. J.* 22 (2019) 1087–1097.
- [14] A.M. Moradi Sizkouhi, S.M. Esmailifar, M. Aghaei, M. Karimkhani, RoboPV: An integrated software package for autonomous aerial monitoring of large-scale PV plants, *Energy Convers. Manag.* 254 (2022) 115217.